Coastal-Trapped Waves on the East Australian Continental Shelf Part II: Model Verification

JOHN A. CHURCH, NEIL J. WHITE, ALLAN J. CLARKE,* HOWARD J. FREELAND,** AND ROBERT L. SMITH†

Division of Oceanography, CSIRO Marine Laboratories, Hobart Tasmania 7001 Australia

(Manuscript received 20 November 1985, in final form 4 August 1986)

ABSTRACT

The Australian Coastal Experiment (ACE) was designed to test coastal-trapped wave (CTW) theory and the generation of coastal-trapped waves by the wind. For the ACE dataset, we use CTW theory to attempt to hindcast the observed alongshelf currents and coastal sea levels at locations remote from the upstream (in the CTW sense) boundary of the ACE region. Local (in the ACE region) wind forcing is responsible for only about a quarter of the CTW energy flux at Stanwell Park (the center of the ACE region), and the remainder enters the ACE region from the south and propagates northward through the ACE region. Including the second-mode CTW improves the correlation between the hindcast and the observed near-bottom currents on the upper slope at Stanwell Park, but the use of the third-mode CTW cannot be justified. A linear bottom drag coefficient of $r = 2.5 \times 10^{-4}$ m s^{-1} works better than a larger drag coefficient, and simplifying the CTW equations by assuming the modes are uncoupled does not detract from the quality of the hindcasts. The hindcast and observed coastal sea levels are correlated at greater than the 99% significance level. For the nearshore locations at Stanwell Park, the hindcast and observed alongshelf currents are correlated at greater than the 99% significance level, and the CTW model can account for about 40% of the observed variance. On the shelf at Stanwell Park, we find the hindcasts agree with the observations only if direct wind forcing within the ACE region and the correct (nonzero) upstream boundary conditions are included. However, even after attempting to remove the effects of the eddies and the East Australian Current, the CTW model is not useful for predicting the currents on the slope at Stanwell Park and on the shelf and slope at Newcastle (the northern boundary of the ACE region). The currents at these locations are dominated by the effect of the East Australian Current and its eddies.

1. Introduction

Since subinertial frequency coastal-trapped waves (CTWs) were first studied in the early 1960s (Hamon, 1962), there have been a number of attempts to use theory to hindcast various aspects of CTWs. The first attempt to use forced wave theory to hindcast continental shelf waves was made by Hamon (1976). He used the barotropic theory of Gill and Schumann (1974) to hindcast sea levels at Evans Head on the east coast of Australia. Hamon (1976) assumed an alongshore phase velocity of 4.0 m s^{-1} [determined from the observed alongshore propagation of sea levels (Hamon, 1966)], but concluded that better agreement between theory and observations would be obtained with a phase velocity of 3.5 to 3.0 m s^{-1}. He also concluded that there was only a small amount of frictional dissipation. The theoretical predictions were of somewhat smaller amplitude than observed, but the amplitude agreement was within a factor of 3 or better. Clarke (1977) showed that the CTW theory could be used to explain, at least qualitatively (and quantitatively for Lake Ontario), a range of observational and numerical results.

Brink (1982) used the CTW theory, with realistic bottom topography and stratification, to predict alongshelf currents off the Peru coast. While the results indicated that the observed variance could only be accounted for if CTWs were present, the quantitative agreement between observed and hindcast currents was not significant over most of the CTW band. More recently, Battisti and Hickey (1984) hindcast sea levels and alongshelf currents for the west coast of the United States. For sea levels, the coherence between observed and hindcast results was significant at the 95% significance level. For alongshelf currents, the agreement was less satisfactory, but the theoretical predictions still accounted for a significant percentage of the variance.

All of these attempts to hindcast observations assumed that the first-mode CTW was dominant. Recently, Mitchum and Clarke (1986) have used up to seven CTW modes to hindcast currents and sea levels on the West Florida Shelf. In Part I of this paper (Church et al. 1986, hereafter referred to as Part I), the second-mode CTW was found to carry at least as much

* Permanent affiliation: Department of Oceanography, Florida State University, Tallahassee, FL 32306.

** Institute of Ocean Sciences, Sidney, British Columbia V8L 4B2, Canada.

† College of Oceanography, Oregon State University, Corvallis, OR 97331.

energy as the first-mode CTW in the dataset obtained for the Australian Coastal Experiment (ACE).

In this paper, we shall use the ACE dataset described in Freeland et al. (1986) to attempt some quantitative tests of the CTW theory. We are not attempting to explain all of the observed variance on the shelf and slope. On the slope, the observed variance is dominated by eddies and the East Australian Current and this makes verification of the theory more difficult. The theory as presented by Clarke and Brink (1985) and Clarke and Van Gorder (1986) is summarized in the Appendix of Part I. This theory includes arbitrary stratification, cross-shelf topography, and linear bottom friction; the waves are assumed to be driven by the alongshelf component of the wind stress or to originate upstream (in the CTW sense) of the ACE region. In section 2, the observations are briefly described and the method of application of the theory of the Appendix of Part I is presented. In section 3, the theory, together with the observed winds and the boundary conditions at the upstream end of the ACE wave guide, is used to hindcast coastal sea levels and alongshelf currents. Correlation and cross-spectral techniques indicate that the hindcasts are significantly coherent with the observations on the shelf and the upper slope. However, the near-surface currents above the slope are dominated by eddies and the East Australian Current, and the theory is unsuccessful at hindcasting these currents. Finally, the usefulness of the model is discussed in section 4.

2. Application of the theory to the ACE dataset

a. The observed currents and pressure and wind stress fields

The main ACE array consisted of three sections of current meters (each with five moorings and each having a total of 15 current meters) offshore from Cape Howe, Stanwell Park and Newcastle (Fig. 1a). The designed placement of the current meters on each section is shown in Fig. 1b. We shall refer to the three sections of current meters as line 1 (Cape Howe), line 2 (Stanwell Park) and line 3 (Newcastle). The current meters are coded as in this example: f23/1000 (f refers to low-pass filtered data) is a meter at a depth of 1000 m on the third mooring from the coast on line 2.

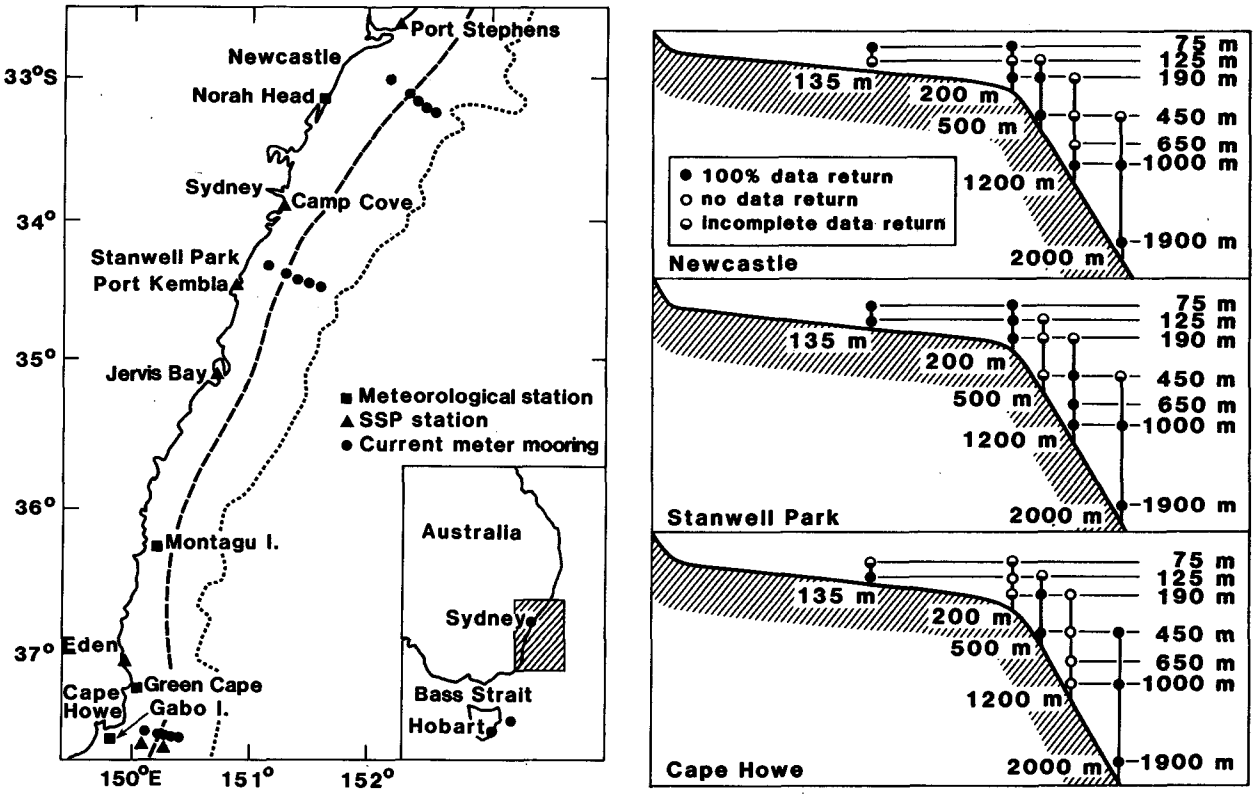

FIG. 1. Location diagram for the Australian Coastal Experiment. (a) The locations of the current meter moorings, SSP records and locations where meteorological data were collected. The sole mooring at 42°40'S on the east coast of Tasmania is shown on the inset. The dashed line is the 200 m isobath and the dotted line is the 4000 m isobath. (b) Schematic (not to scale) diagram of the locations of current meters on the sections at Cape Howe, Stanwell Park and Newcastle. A solid circle indicates 100% data return, an open circle zero data return, and a half shaded circle indicates an incomplete record.

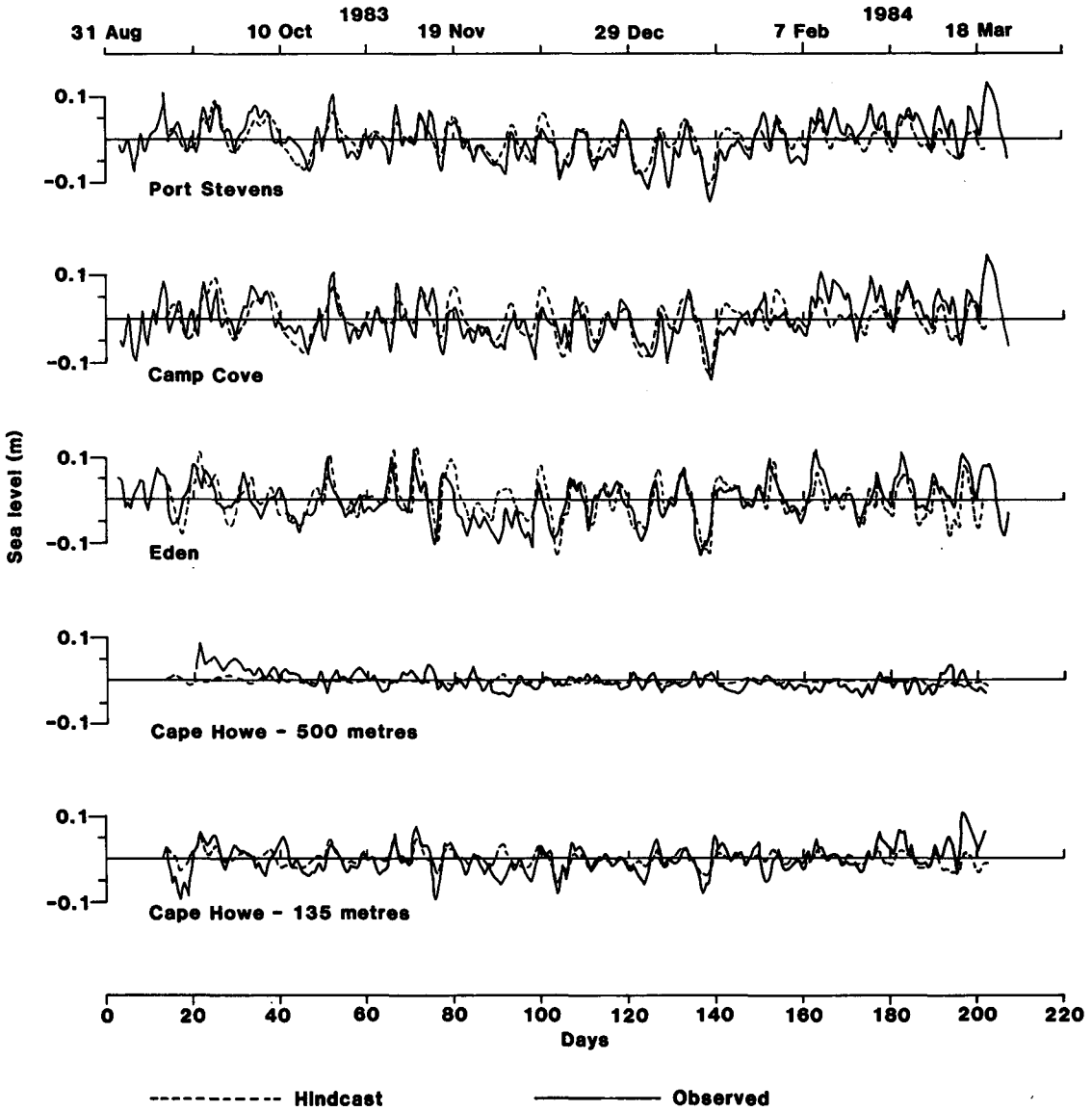

FIG. 2. Comparison of hindcast and observed sea levels.

The details of the preliminary data analysis are given in Part I and Freeland et al. (1985). Briefly, the data was bandpassed to remove periods greater than 24 days and less than 2 days, and only the alongshelf component of the current was used.

Coastal subsurface pressure (SSP) data are available at Eden, Jervis Bay, Port Kembla, Camp Cove and Port Stephens (Fig. 1). SSP data are also available at the bottom of the 135 and 500 m moorings at Cape Howe; they are referred to as fp11 and fp13, respectively. Details of the data and data processing are given in Forbes (1985a). As with the current meter data, the series were bandpassed.

Meteorological data were obtained for 16 Bureau of Meteorology stations and for three buoys moored at midshelf. From this dataset, we selected three stations that provided continuous data during ACE and which we considered to be representative of the wind stress field. These stations, at Green Cape, Montagu Island and Norah Head (Fig. 1), were used in the application of the CTW theory. Full details of the data and the wind field over the ACE region are given in Forbes (1985b and personal communication, 1985).

b. Application of the theory

To hindcast the alongshelf currents and coastal sea levels, it is first necessary to know the amplitude ϕ of the CTW modes at the upstream end of the wave guide. In Part I, these amplitudes of the CTW modes were found by solving

TABLE 1. Observed and hindcast variance for the SSPs and the correlation coefficient between these two signals. The record is incomplete for the stations marked with an asterisk.

Location	Observed variance $(cm)^2$	Hindcast variance $(cm)^2$	Correlation coefficient
fp13	6.3	0.4	0.23
fp11	16.0	4.6	0.54
Eden	32.8	30.0	0.64
Jervis Bay*	25.4	30.4	0.66
Port Kembla*	43.9	26.6	0.60
Camp Cove	31.1	24.9	0.63
Port Stephens	30.9	17.6	0.75

$$\mathbf{G}\phi = \mathbf{v}, \tag{2.1}$$

where the njth element of the matrix **G** is the alongshelf current component of the jth eigenfunction at the nth ($n \leq 15$) current meter location at Cape Howe. Because of the finite quantity of data and the presence of other phenomena besides CTWs (such as East Australian Current eddies), only the amplitude of the first three CTW modes was estimated. To minimize contamination from the East Australian Current, a statistical "eddy" mode (see Part I) was defined and included in the analysis so that **G** consisted of four column vectors. As this analysis was completed at all three sections, the modal amplitudes are known at Cape Howe, Stanwell Park and Newcastle.

The theory outlined in the Appendix of Part I was then used to step along the coast. In completing this hindcast, we allow the eigenfunctions F_j (for the pressure field) (and hence G_j for the velocity field), the phase speeds c_j, and the coupling coefficients b_j and a_{ij} to vary with the alongshelf location. All of these parameters were evaluated for the Cape Howe, Stanwell Park and Newcastle sections and linearly interpolated for locations between the sections. The eigenfunctions and eigenvalues were computed for the estimated topography and Brunt–Väisälä frequency profiles (see Part I for details) using the methods of Brink and Chapman (1985). The first-mode phase velocities increase from 3.2 m s^{-1} at Cape Howe to 4.0 m s^{-1} at Stanwell Park and to 5.2 m s^{-1} at Newcastle. The increase is due to the increased stratification in the north and also to the increased shelf width. Sensitivity tests indicated that the eigenfunctions and the phase velocities were not

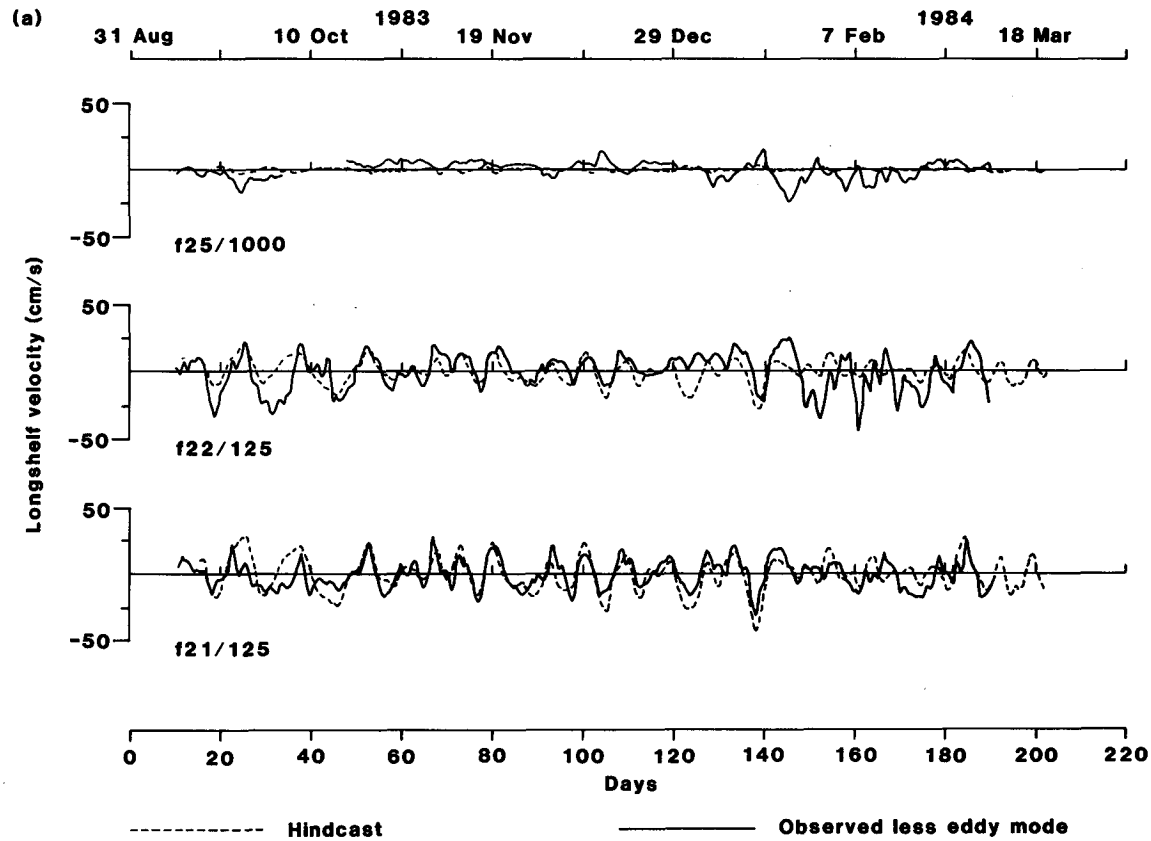

FIG. 3. Comparison of the hindcast alongshelf current with the de-eddied observations for (a) Stanwell Park and (b) Newcastle. The predictions were completed with a model using three CTW modes. The observations have been band-passed and the effects of the eddy mode removed [Eq. (4.1)]. Only a representative selection of current meter records is presented.

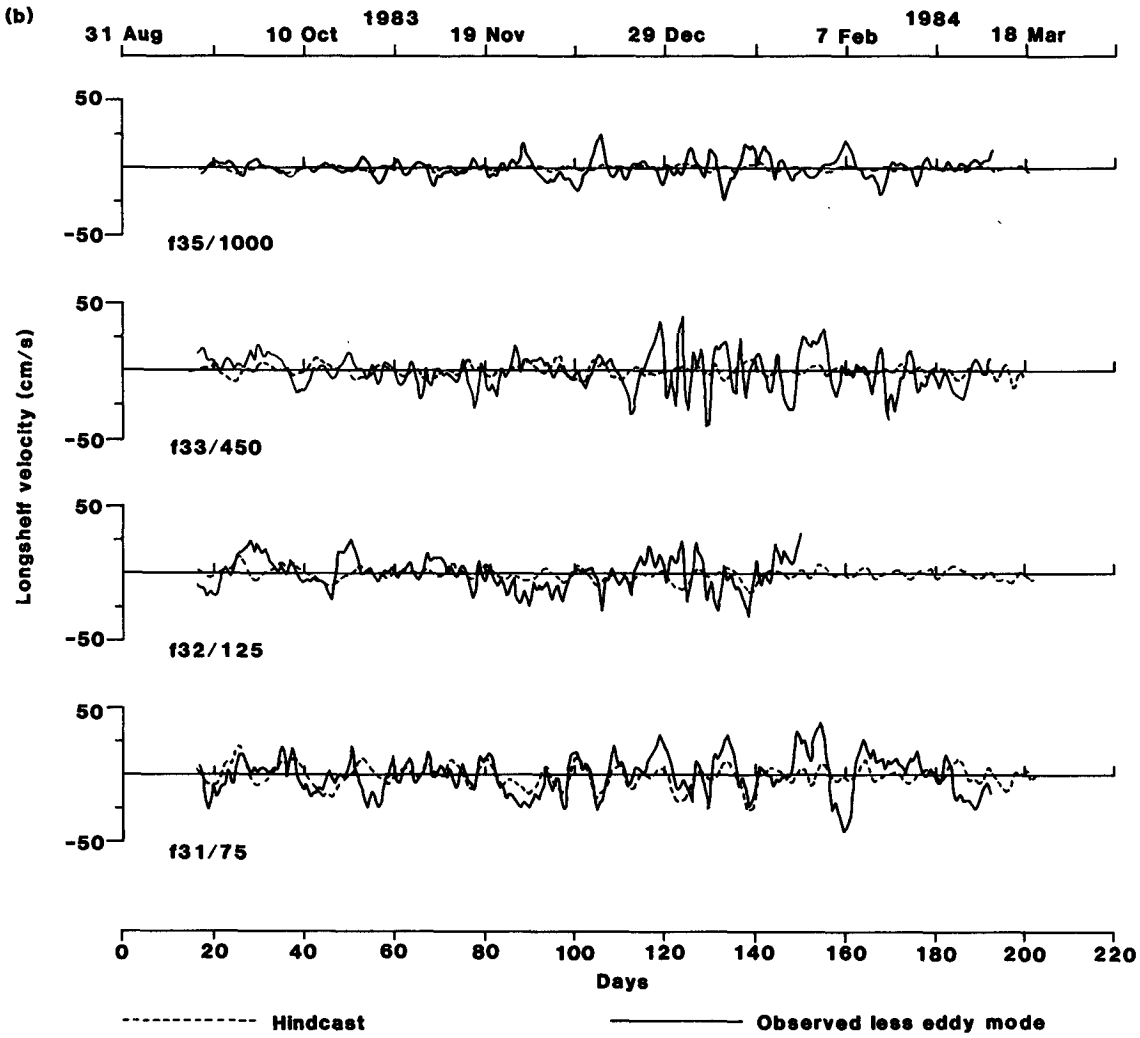

FIG. 3. (*Continued*)

sensitive to small changes in the depth or the stratification profiles (such as might be produced by inaccuracies in the data or local variations in the shelf conditions), but that for accurate quantitative results it is necessary to allow for gross changes in $h(x)$ and $N^2(z)$ that occur between current meter sections.

The frictional coupling coefficients were evaluated using linear bottom friction evaluated from $r = C_D U_S$. A value of 0.0025 was used for the bottom drag coefficient C_D, and a value of 0.2 m s^{-1} for the scale velocity U_s, which implies that $r = 5 \times 10^{-4}$ m s^{-1}. The value of r was taken to be independent of the cross-shelf coordinate.

Wind stress was calculated from the observed winds at Green Cape, Montagu Island and Norah Head (Fig. 1) using the neutral steady state drag coefficient of Large and Pond (1981).

The wave band we shall consider is that associated with synoptic weather events with periods ranging from a few days to a few weeks. In particular, the lowest frequency motion we consider has a period of 24 days and the highest frequency has a period of 3.7 days.

3. Comparison of observed and modeled coastal-trapped waves

a. Sea levels

The SSPs and alongshelf velocities observed during ACE were hindcast using the theory outlined in the Appendix of Part I, the boundary conditions (at Cape Howe) determined in Part I, and the observed winds. The hindcast and observed SSPs are compared in Fig. 2 and Table 1. For the pressure record at the most southerly location on the coast (Eden), the hindcast and observed SSPs are of comparable magnitude and are significantly correlated at above the 99% significance level. We calculated the integral time scales following Davis (1976). If Eden and Camp Cove sea levels are used, the integral time scale is 5 days (as used by

TABLE 2. Correlation coefficients between the de-eddied observed alongshelf currents and the hindcast currents at Stanwell Park and Newcastle. The correlation coefficients are given for the total ACE period and, for Stanwell Park, are also given for the period when no eddies were present (days 50 to 140).

	Stanwell Park		Newcastle	
Location	Correlation coefficient (complete record)	Correlation coefficient (days 50–140)	Location	Correlation coefficient (complete record)
f21/75	0.43	0.76	f31/75	0.45
f21/125	0.65	0.79	f31/125	0.63
f22/75	0.29	0.52	f32/75	0.39
f22/125	0.40	0.60	f32/125	0.33
f22/190	0.49	0.62	f32/190	0.13
f23/125	0.57	No data	f33/25	0.22
f23/190	0.20	No data	f33/190	0.18
f23/450	−0.07	No data	f33/450	0.17
f24/170	0.02	0.41	f34/190	−0.02
f24/450	−0.04	0.28	f34/450	−0.16
f24/650	−0.04	0.00	f34/650	0.06
f24/1000	0.36	0.36	f34/1000	0.35
f25/450	−0.28	0.18	f35/450	0.03
f25/1000	0.22	0.18	f35/1000	0.21
f25/1900	0.15	0.17	f35/1900	−0.10

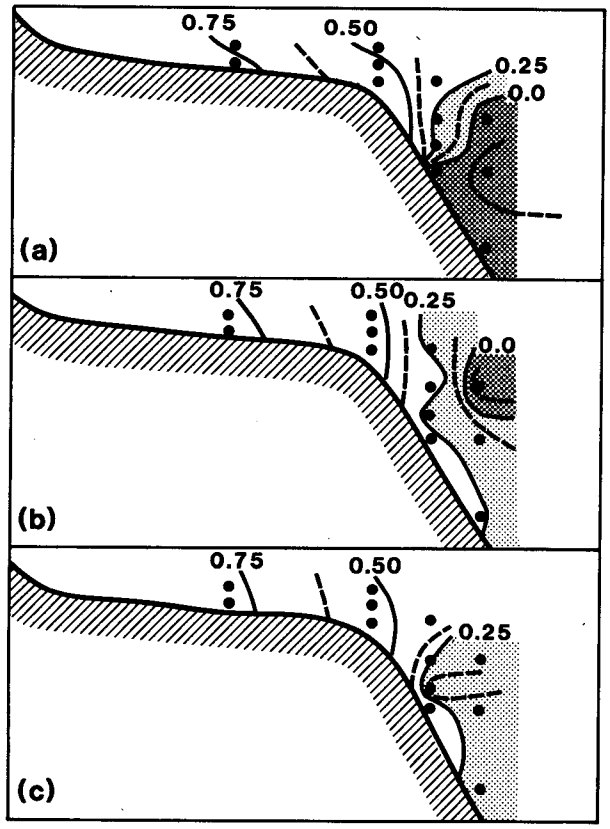

FIG. 4. Contour plot of the correlation between the hindcast alongshelf current and the de-eddied observations between days 50 and 140. Only one CTW mode is used in (a), two CTW modes are used in (b), and three CTW modes are used in (c). Regions of negative correlation are indicated by heavy stippling; light stippling indicates regions where the correlation coefficient is less than 0.25 but greater than zero.

Freeland et al., 1986). However, if the currents at f11/125 and f21/125 are used, the integral time scale is about 3 days. To estimate significance levels, we have used the more conservative time scale of 5 days, and thus for a record length of 180 days and an integral time scale of 5 days the 95% significance level is 0.325 and the 99% significance level is 0.418. In contrast, for the record at the 500 m isobath (fp13), both the observed and hindcast signals are small (as is expected for CTWs) and are not significantly correlated. At midshelf (the 135 m isobath—fp11), the observed and hindcast series are of intermediate magnitude (compared to Eden and fp13) and are significantly correlated. For the coastal SSP at Camp Cove and Port Stephens (the two other sites with complete records), the hindcast and observed series have similar variances and are significantly correlated at greater than the 99% significance level (Table 1).

Although we have used only the velocities at Cape Howe to determine the amplitudes of the CTW modes, the model can successfully hindcast the observed SSP at the northern limit of the ACE array. It is also apparent (Fig. 2) that the comparison is poorer at some times than others. This is at least partially due to the presence of offshore eddies that are affecting the coastal sea levels, which, as we shall see, have an even more marked effect on the alongshelf currents.

b. Currents

In comparing the hindcast alongshelf currents with the observations, it must be remembered that offshore events (eddies and the East Australian Current) strongly affect the currents on the shelf and that CTWs only

account for a fraction of the observed variance. In Part I, an attempt was made to minimize the contamination of the CTW mode amplitudes by including a statistical eddy mode in the least-squares fit. For an initial comparison of hindcast currents with the observations, we have attempted to remove that part of the current due to eddies by generating a "de-eddied" current $\mathbf{v}^{de}$ given by

$$v_n^{de} = v_n - G_{n4}\phi_4. \tag{3.1}$$

Note that v_n^{de} includes the contribution from the first three CTW modes and a residual noise factor ϵ, which could include contributions from higher-order CTW modes and from the East Australian Current.

This de-eddied current is compared with a representative range of hindcast currents at Stanwell Park and Newcastle in Fig. 3. The correlation coefficients (Table 2) are largest for the nearshore meters, where the hindcast and observed variances are of a similar magnitude, and the correlation coefficients gradually decrease with increasing distance from the coast. The variance in both the observed and hindcast series decreases with increasing distance beyond the shelf break, with the hindcast variance decreasing faster than the observed variance. This result is not surprising given that CTWs are trapped on the continental shelf and slope, and the presence of East Australian Current eddies in the offshore region. Also, the correlation coefficients are larger for Stanwell Park than for Newcastle. This is because of the small amount of variance accounted for by the first three CTW modes at Newcastle (See Part I). As for the sea levels, the correlation coefficients for the nearshore velocities are well above the 99% significance level of 0.418 (Table 2).

Offshore, the correlations are not significant at the 95% level. Due to the effects of eddies, there are periods when the hindcast is significantly worse than at other times; i.e., while we have reduced the effects of eddies on the currents by using a statistical eddy mode, we have not entirely removed their effects. In fact, there are periods (particularly from late January to February at Stanwell Park) when the eddies dominate the observed currents at all locations across the shelf. In contrast, for the period between days 50 and 140, other observations (CTD data, XBT data, satellite-tracked buoys and satellite infrared images) taken during ACE indicate that no large eddies were affecting the currents at Stanwell Park. The correlations for this period are considerably higher than they are for the complete ACE period (Table 2); in the offshore region all the correlations are positive and some are significant at the 95% level.

We have attempted to answer the question "How many CTW modes are necessary to hindcast the observed currents successfully?" For this test, we concentrated on the alongshelf currents at Stanwell Park for the period between days 50 and 140 when eddies were absent from the Stanwell Park region. We repeated the fitting of CTW modes at Cape Howe and the subsequent hindcasting of alongshore velocities at Stanwell Park using two rather than three CTW modes, and one rather than three CTW modes, and compared the results with the de-eddied currents at Stanwell Park. For the locations on the shelf, including only two modes gives marginally higher correlations than including three modes, which in turn gives higher correlations than including only one mode. However, for locations 24/1000, 24/450, 25/1000 and 25/1900, using only one mode (Fig. 4) resulted in negative correlations; i.e., one mode cannot account for the observed reversal of sign of the longshore currents. In contrast, when two modes were used, the only negative correlation was at 25/450, and for three modes all correlations were positive.

In Part I, it was found that CTWs accounted for only a fraction of the observed variance and that even when an eddy mode was included some variance was still unaccounted for. We also found that removing the eddy mode from the observations did not remove all of the eddy signal from the data. To avoid this noise, we applied a more realistic test of CTW theory by comparing the predictions with currents we believe to be associated with CTWs. At Stanwell Park and Newcastle sections, we define reconstructed currents as

$$v_n^r = \sum_{j=1}^{3} G_{nj}(x, y)\phi_j(y, t) \tag{3.2}$$

where ϕ_j is determined from the data (see Part I). Since Eq. (3.2) involves a summation limited to the first three CTW modes, the reconstructed currents are due to the dynamical modes with a relatively small amount of contamination from eddies of from other phenomena; i.e., the residual noise factor ϵ is not included in Eq. (3.2) whereas it is included in Eq. (3.1). A comparison of the reconstructed currents with the hindcast velocities is shown in Fig. 5 and Table 3. Compared to the correlations for the de-eddied currents, the correlation between the two signals is only marginally different near the coast but is significantly improved offshore.

The time series of the amplitudes of modes 1, 2 and 3 at Stanwell Park, as calculated from the observations and as hindcast from the above theory, are shown in Fig. 6. The correlation coefficients between the observed and hindcast time series are 0.47 and 0.51, respectively, for modes 1 and 2 at Stanwell Park; for mode 1 at Newcastle the correlation coefficient is 0.44. The correlation coefficients for mode 3 are not significant for either location, and for mode 2 the correlation coefficient is not significant for Newcastle. Cross spectra (Fig. 7) between observed and hindcast series at Stanwell Park indicate that for mode 1 the series are significantly correlated for all periods, except 4.8 days over the 24 to 3.7 day wave band, and there is a near zero phase difference for the entire wave band. The

transfer function is about 1.2 for periods of 8 and 6 days, but is about 0.7 for the rest of the wave band. These estimates of the transfer function are not significantly different from unity. For mode 2, the series are significantly correlated over the entire wave band and there is a near zero phase difference for periods from 24 to 4.8 days; however, at a period of 3.6 days this phase difference suddenly jumps to 180°. The transfer coefficient ranges from 0.4 for a period of 3.6 days to 0.7 at a period of 6 days; i.e., the hindcast series is too small by about 40%. For mode 3, the series are not significantly correlated in the wave band.

To estimate the sensitivity of the solution to variations in the friction coefficients, we arbitrarily halved and doubled the frictional coupling coefficients a_{ij}. When the coupling coefficients were doubled (increased friction), the coherences fell slightly and the phase lags increased by 10° to 20°. However, the transfer function decreased by between 10% and 50% for mode 1 and by between 20% and 50% for mode 2. When the coupling coefficients a_{ij} were halved, the transfer coefficients for mode 1 increased for periods greater than 6 days but were smaller for higher frequencies. For mode 2, the transfer function increased by about 20% to a range from 0.64 to 0.9 for periods greater than 3.6 days. The final sensitivity test was to set the off-diagonal terms of the matrix of frictional coupling coefficients (a_{ij}) equal to zero. This approach greatly simplifies Eq. (2.3) in that it decouples the modes, and one equation can be solved for each mode rather than a set of coupled equations. The cross spectra for this case are also shown in Fig. 7. The mode 2 transfer function is marginally closer to unity, but otherwise the results are not significantly different from the standard case.

4. Discussion

The theoretical frictional space (and time) decay scales used in the model for modes 1, 2 and 3 for the Stanwell Park section are 1800 km (5.2 days), 1200 km (6.5 days) and 1100 km (10 days), respectively. Mode 3 (and higher-order modes) have a shorter decay distance than mode 1, and in Part I it was shown that the observed modal amplitudes for mode 3 were not coherent between any pair of sections. Moreover, the hindcast and observed mode 3 amplitudes were not

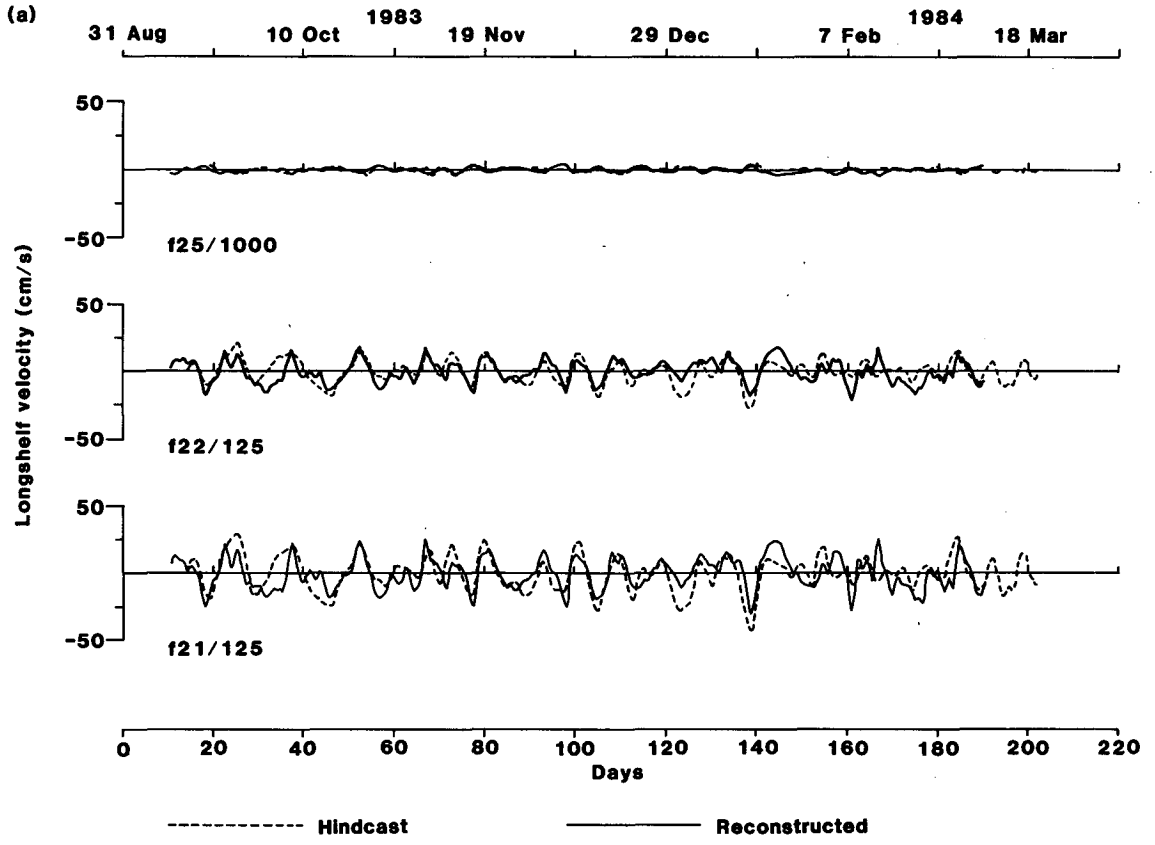

FIG. 5. Comparison of the hindcast alongshelf currents with the reconstructed currents at (a) Stanwell Park and (b) Newcastle. The predictions were completed using a model using three CTW modes, and Eq. (4.2) was used for the reconstructed velocities. Only a representative selection of current meter records are presented.

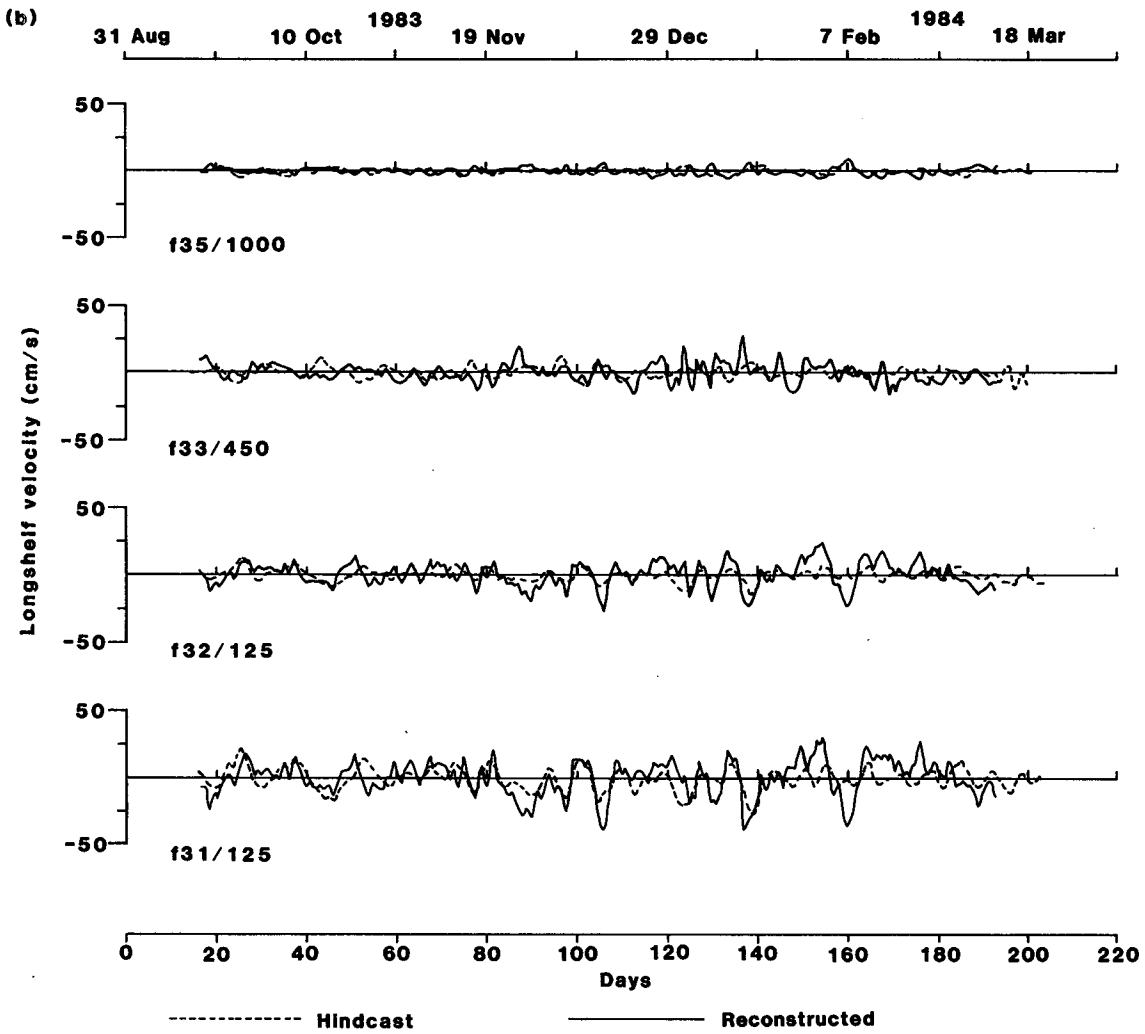

FIG. 5. (*Continued*)

coherent, and it is unlikely that higher order modes can be identified with most practical instrument arrays. For these reasons, mode 3 (and higher order modes) are not very useful in ACE for a hindcast of alongshelf currents. However, at least two modes are necessary to hindcast the currents on the upper slope at Stanwell Park. For nearshore locations where friction becomes relatively more important, the inclusion of higher order modes may be necessary.

The attempts to hindcast the observations using a CTW model indicated that halving the friction parameter to $r = 2.5 \times 10^{-4}$ m s^{-1} gave a transfer function closer to the theoretically expected value of unity. This conclusion agrees with Battisti and Hickey (1984), who found that a decay time scale of 5 days or longer worked best. Also, Hamon (1976) found higher correlations between hindcast and observed sea levels on the east Australian coast when he used a relatively small friction parameter. Note that even when the friction parameter is reduced by a factor of 2, the decay time scales for the CTW modes are on the order of the period of the waves, and they will decay substantially before they have propagated one wavelength; the CTWs are heavily damped. Despite this heavy damping, CTWs can carry energy substantial distances (perhaps 1000 or 2000 km). For a number of continental shelves, strong forcing is remote and upstream (in the CTW sense) from the region of interest; i.e., the CTWs are mainly freely propagating through the region of interest. The ACE region and the shelf off Peru (Brink, 1982) are two regions where remote forcing is important.

Assuming that the modes are uncoupled does not appear to detract from the quality of the hindcasts. Since this greatly simplifies the problem, it seems preferable to assume that the CTW modes are uncoupled. These conclusions could possibly change if different

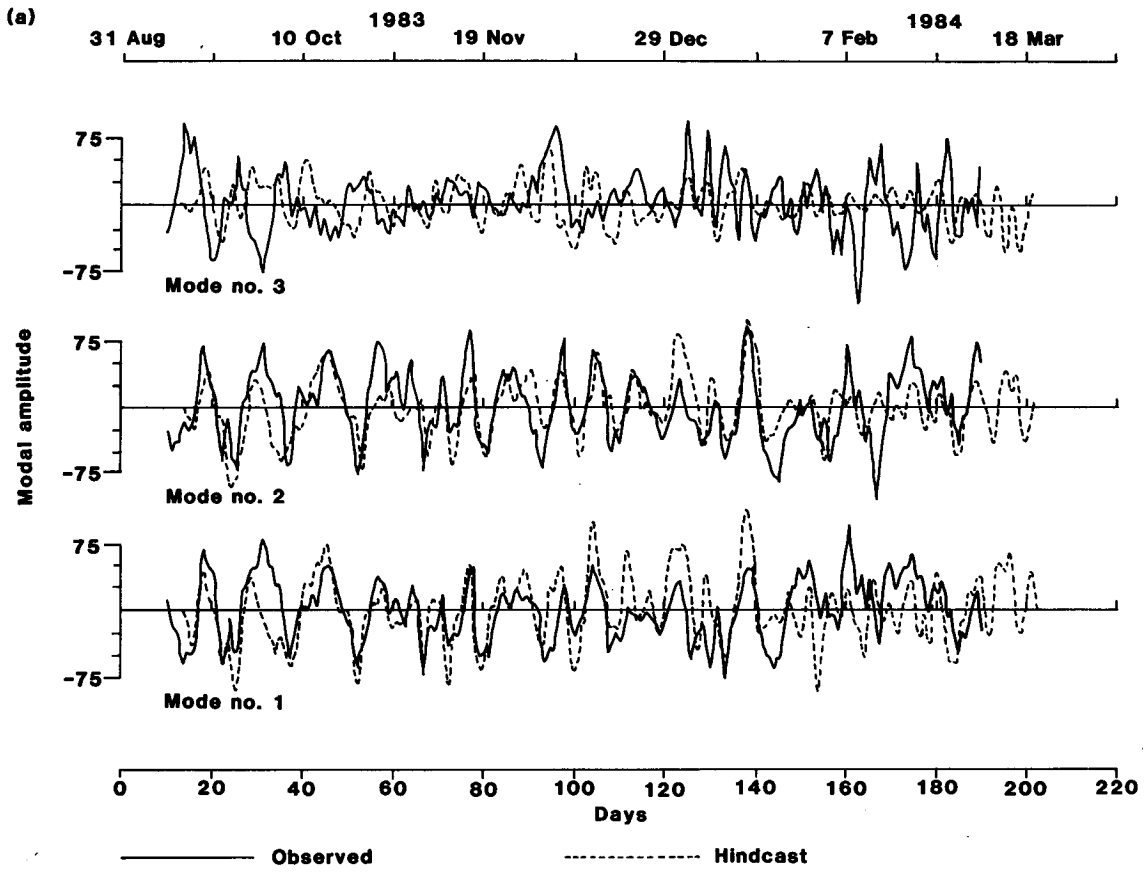

FIG. 6. Comparison of the first three CTW mode amplitudes as estimated from the observations and hindcast by the model at (a) Stanwell Park and (b) Newcastle.

distributions of bottom friction, as might be induced by surface waves or other phenomena, were assumed.

Given that we found that the hindcast and observed SSPs and alongshelf currents were highly coherent on the shelf at Stanwell Park, how well does the coastal-trapped wave theory work as a predictive tool? For the

TABLE 3. Correlation coefficients between the "reconstructed" alongshelf currents and the hindcast currents at Stanwell Park and Newcastle. The correlation coefficients are given for the total ACE period and, for Stanwell Park, are also given for the period when no eddies were present (days 50 to 140).

	Stanwell Park		Newcastle	
Location	Correlation coefficient (complete record)	Correlation coefficient (days 50–140)	Location	Correlation coefficient (complete record)
f21/75	0.62	0.74	f31/75	0.50
f21/125	0.62	0.74	f31/125	0.50
f22/75	0.61	0.74	f32/75	0.49
f22/125	0.61	0.73	f32/125	0.47
f22/190	0.55	0.69	f32/190	0.17
f23/125	0.50	0.66	f33/125	0.36
f23/190	0.36	0.55	f33/190	0.20
f23/450	0.00	0.26	f33/450	0.19
f24/190	0.23	0.45	f34/190	0.18
f24/450	0.01	0.27	f34/450	0.23
f24/650	0.24	0.45	f34/650	0.32
f24/1000	0.51	0.57	f34/1000	0.22
f25/450	0.10	0.35	f35/450	0.25
f25/1000	0.42	0.50	f35/1000	0.15
f25/1900	0.07	0.18	f35/1900	−0.08

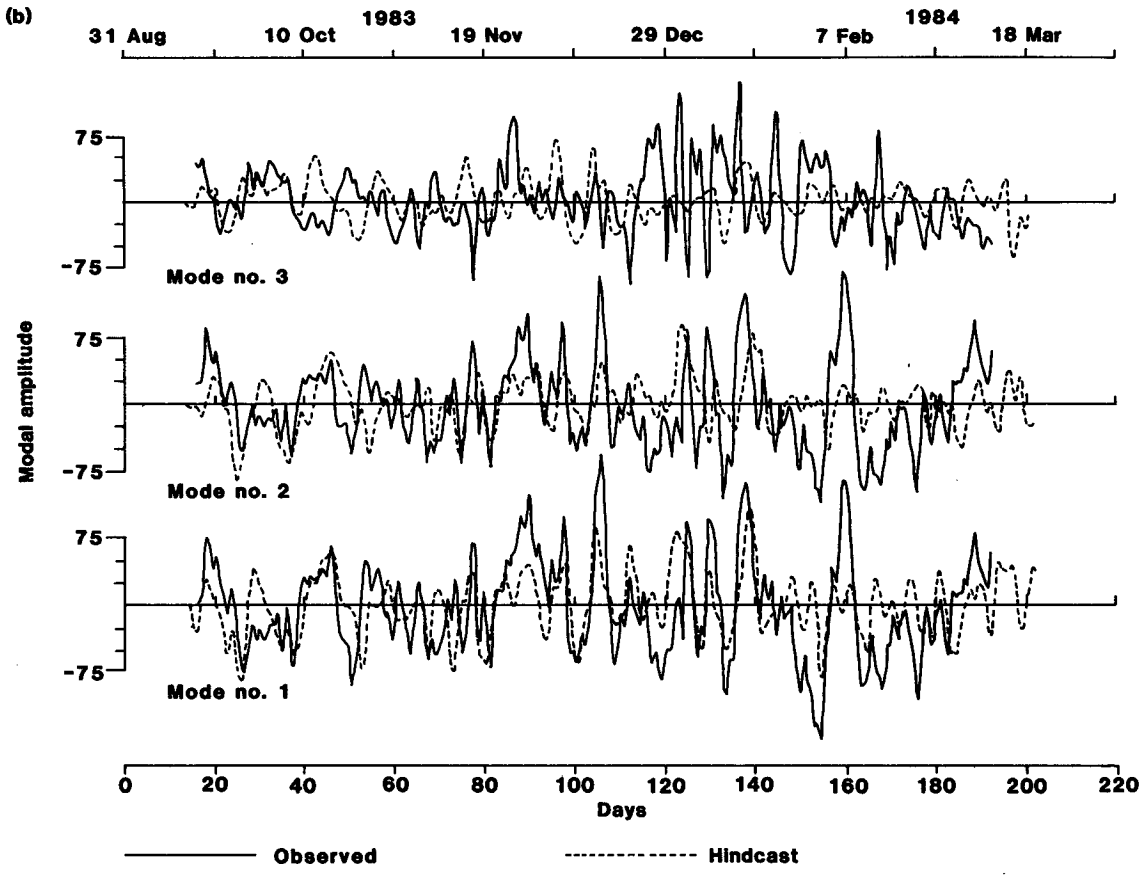

FIG. 6. (*Continued*)

nearshore current meters at Stanwell Park, we have calculated the residual variance (i.e., we subtracted the hindcast alongshelf currents from the observed alongshelf currents and calculated the variance of this residual). For the periods when eddies were not present, the observed variances for meters f21/75 and f21/125 are 114 and 131 $cm^2\ s^{-2}$, respectively, while the residual variances are 69 and 72 $cm^2\ s^{-2}$, respectively. These residual variances are 61% and 55% of the observed variances, so for these nearshore regions the CTW model is a practical tool for estimating the alongshelf currents. Further offshore and at Newcastle, the predictions are not useful because eddies and the East Australian Current dominate. Closer to shore, where the East Australian Current eddies have less effect, one would expect the CTW model to do somewhat better than further offshore. An alternative predictive model would be to assume that, because shelf currents generally have a large alongshelf scale, the currents at Cape Howe are identical to those at the corresponding location at Stanwell Park. However, examination of records f11/125 and f21/125 shows that at zero lag the correlation coefficient is only 0.29 (in contrast to 0.74; Table 3), and if f11/125 is used as a predictive tool for f21/125 then the residual variance is larger than the variance of f21/125.

In contrast to the situation at Stanwell Park, the East Australian Current and its eddies dominate currents offshore from Newcastle, and for the observation locations the CTW model is not a useful predictive tool.

The dominant energy source for the observed coastal-trapped waves does not lie in the ACE region; i.e., it is not the "local" wind that is dominant in driving the currents on the shelf. If the amplitudes of the CTWs at Cape Howe are set to zero, then the energy fluxes predicted for Stanwell Park are too small by about a factor of 3 for mode 1 and about a factor of 7 for mode 2. Similarly, when the correct upstream boundary conditions were used but the winds within the main ACE region were set to zero, the energy flux at Stanwell Park was too small by about a factor of 2 for mode 1 and a factor of about 3 for mode 2. When both the correct boundary conditions and the winds were used, the energy flux at Stanwell Park was too large by about 20% for mode 1 and too small by about 35% for mode 2. It appears that about three-quarters of the CTW signal observed at Stanwell Park is the result of free propagation from Cape Howe and the remainder due to wind

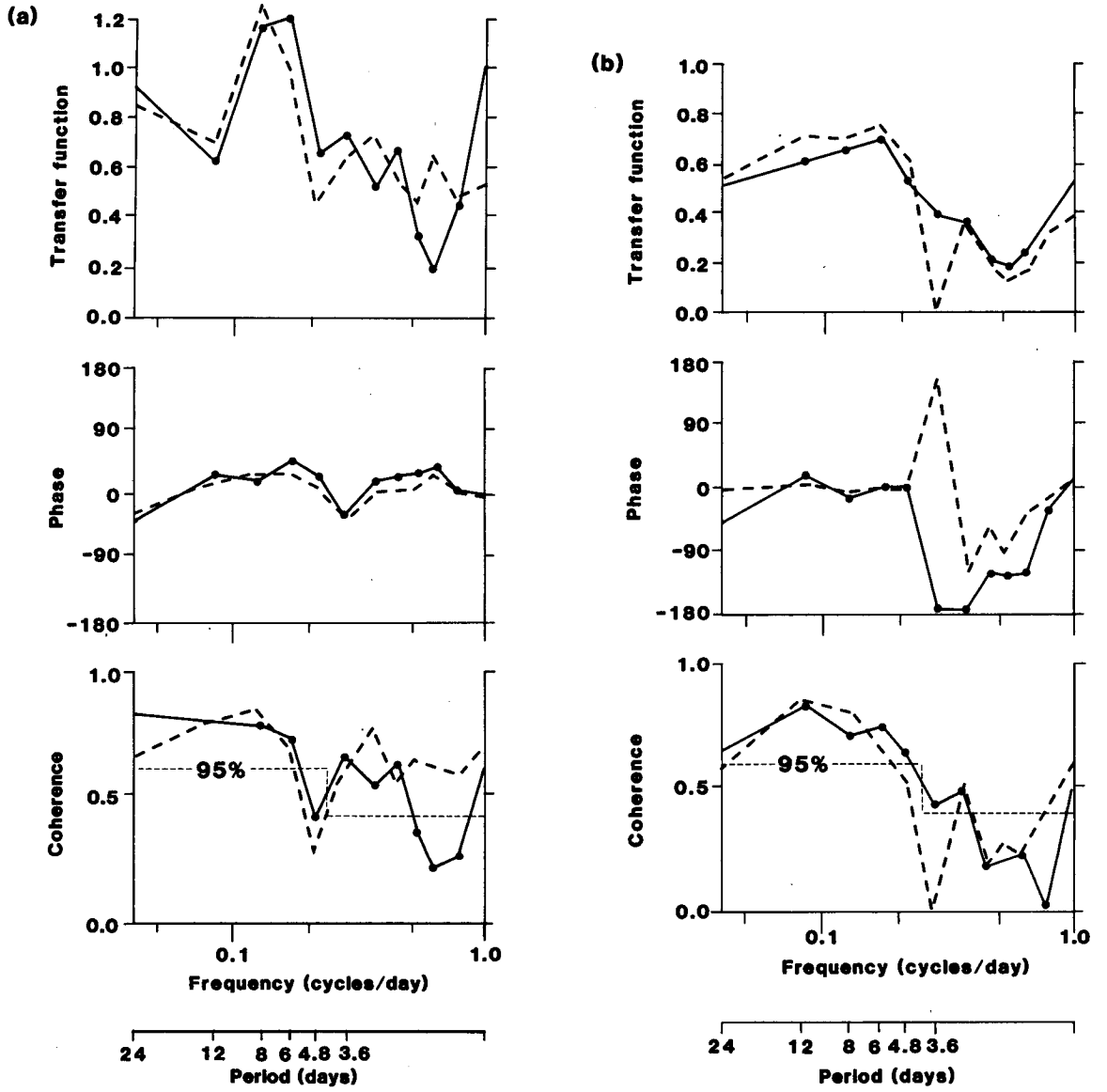

FIG. 7. Cross spectra between the amplitude of the CTW modes calculated from the observations at Stanwell Park and hindcast using the CTW model. Mode 1 is shown in (a) and mode 2 in (b). The solid line is the standard case and the dashed line is assuming the matrix (a_{ij}) is diagonal. The 95% significance level is indicated by the dotted line.

forcing north of Cape Howe. To successfully hindcast the observations, both the correct boundary conditions and the correct winds are necessary. The free wave assumption implicit in the analysis of Freeland et al. (1986), and in Part I, works well because the CTWs are dominated by free rather than forced waves, and as Clarke and Thompson (1984) showed, the response forced by a reasonable distribution of wind stress in the ACE region appears to propagate at speeds not greatly different from the phase speeds of the free waves.

While Hamon (1976) found high coherence between sea levels at Evans Head (29°S) and results from the Gill and Schumann (1974) model, the gain between the model results and the observations was somewhat larger than the expected value of unity. It appears that the likely explanation for this result is that Hamon (1976) assumed (in contradiction to the present results) that there was no CTW energy propagating past Gabo Island and that the response at Evans Head was due to wind forcing between Gabo Island and Evans Head.

A substantial fraction of the energy for the observed CTWs must be input into the coastal-wave guide south and west of Cape Howe. One possibility is that the very strong winds at and just to the south and west of Cape Howe generated the observed signals. Forbes (personal communication, 1985) found that for Gabo Island the

wind-stress rms variance during the ACE period was 0.31 N m^{-2}. This hypothesis was tested by using the Gabo Island winds over the 150 km between Cape Howe and the eastern extremity of Bass Strait to drive the CTW model. For the nearshore locations, the coherences between observed and hindcast currents were up to 0.68 (compared with 99% significance level of 0.418). However, the energy flux at Cape Howe calculated in this model was about a factor of 4 too small for mode 1 and about a factor of 5 too small for mode 2. As pointed out by Freeland et al. (1986), not much CTW energy is propagated past the sole mooring off the eastern coast of Tasmania. However, another alternative discussed by Freeland et al. (1986) is that the CTW energy is generated in Bass Strait or on the east coast of Tasmania (north of the sole mooring at 42°40′S). If the winds measured at Gabo Island are representative of winds over the entire region, then this solution is certainly possible. A wind-generated east–west flow through Bass Strait would experience rapid topographic variations at the eastern end of Bass Strait, which might allow the generation of the second (and higher order) CTW modes as observed at Cape Howe. Theoretical work (e.g., Allen, 1976) does allow the possibility of the scattering of energy from a first-mode continental shelf wave to higher-order modes. Recent theoretical work (Buchwald and Kachoyan, personal communication, 1985) has shown that an eastward flow through Bass Strait does generate higher order CTWs on the east coast and that almost all of this energy travels to the north through the ACE region. Recent observational work (Church and Freeland, 1986) has shown that sea levels are highly correlated right across the south coast of Australia, through Bass Strait, and into the ACE region. These two pieces of work suggest that it is the strong wind on the south coast of Australia which is the predominant driving force for the CTWs on the south east Australian continental shelf.

Acknowledgments. ACE was initiated and encouraged by Rory Thompson. We also thank him for critical comments on drafts of this paper. The participation of Oregon State University in ACE was supported by the U.S. Office of Naval Research. Support for Allan J. Clarke was received from the U.S. National Science Foundation (Grant OCE-8300029). The participants from North America, Howard J. Freeland, Allan J. Clarke and Robert L. Smith, would like to thank the CSIRO for its hospitality during the data analysis phase of the experiment. Finally, we would like to thank Bernadette Baker and Nikki Pullen for their patience in typing the many drafts of this paper.

REFERENCES

Allen, J. S., 1976: Continental shelf waves and alongshore variations in bottom topography and coastline. *J. Phys. Oceanogr.*, **6,** 864–878.

Battisti, D. S., and B. M. Hickey, 1984: Application of remote wind-forced coastal trapped wave theory to the Oregon and Washington coasts. *J. Phys. Oceanogr.*, **14,** 887–903.

Brink, K. H., 1982: A comparison of long coastal trapped wave theory with observations off Peru. *J. Phys. Oceanogr.*, **12,** 897–913.

——, and D. C. Chapman, 1985: Programs for computing properties of coastal-trapped waves and wind-driven motions over the continental shelf and slope. Woods Hole Oceanographic Institute Tech. Rep. WHOI-85-17, 99 pp.

Church, J. A., and H. J. Freeland, 1986: The energy source for the coastal-trapped waves in the Australian Coastal Experiment region. *J. Phys. Oceanogr.*, in press.

——, —— and R. L. Smith, 1986: Coastal-trapped waves on the east Australian continental shelf. Part I: Propagation of modes. *J. Phys. Oceanogr.*, **16,** 1929–1943.

Clarke, A. J., 1977: Observations and numerical evidence for wind-forced coastal-trapped long waves. *J. Phys. Oceanogr.*, **7,** 231–247.

—— and R. O. R. Y. Thompson, 1984: Large-scale wind-driven ocean response in the Australian Coastal Experiment region. *J. Phys. Oceanogr.*, **14,** 338–352.

—— and K. H. Brink, 1985: The response of stratified, frictional shelf and slope waters to fluctuating large-scale low-frequency wind forcing. *J. Phys. Oceanogr.*, **15,** 439–453.

—— and S. Van Gorder, 1986: A method for estimating wind-driven frictional, time-dependent, stratified shelf and slope water flow. *J. Phys. Oceanogr.*, **16,** 1013–1028.

Davis, R. E., 1976: Predictability of sea surface temperature and sea level pressure anomalies over the North Pacific Ocean. *J. Phys. Oceanogr.*, **6,** 249–266.

Forbes, A. M. G., 1985a: Sea-level data from the Australian Coastal Experiment—a data report. CSIRO Marine Lab. Rep. No. 171, 16 pp.

——, 1985b: Meteorological data from the Australian Coastal Experiment—a data report. CSIRO Marine Lab. Rep. No. 170, 26 pp.

Freeland, H. J., J. A. Church, R. L. Smith and F. M. Boland, 1985: Current meter data from the Australian Coastal Experiment; a data report. CSIRO Marine Lab. Rep. No. 169, 51 pp.

——, F. M. Boland, J. A. Church, A. J. Clarke, A. M. G. Forbes, A. Huyer, R. L. Smith, R. O. R. Y. Thompson and N. J. White, 1986: The Australian Coastal Experiment: A search for coastal-trapped waves. *J. Phys. Oceanogr.*, **16,** 1230–1249.

Gill, A. E., and E. H. Schumann, 1974: The generation of long shelf waves by the wind. *J. Phys. Oceanogr.*, **4,** 83–90.

Hamon, B. V., 1962: The spectrums of mean sea level at Sydney, Coff's Harbour, and Lord Howe island. *J. Geophys. Res.*, **67,** 5147–5155. [Correction, *J. Geophys. Res.*, **68,** p. 4635.]

——, 1966: Continental shelf waves and the effects of atmospheric pressure and wind stress on sea level. *J. Geophys. Res.*, **71,** 2883–2893.

——, 1976: Generation of shelf waves on the East Australian coast by wind stress. *Mem. Soc. R. Sci. Liege, Ser. 6.*, **X,** 359–367.

Large, W. S., and S. Pond, 1981: Open ocean momentum flux measurements in moderate to strong winds. *J. Phys. Oceanogr.*, **11,** 324–336.

Mitchum, G. T., and A. J. Clarke, 1986: Evaluation of frictional, wind forced long-wave theory on the West Florida Shelf. *J. Phys. Oceanogr.*, **16,** 1029–1037.